Neurobiology of Aging 35 (2014) 1660–1668

Contents lists available at ScienceDirect

Neurobiology of Aging

journal homepage: www.elsevier.com/locate/neuaging

Longitudinal neurochemical modifications in the aging mouse brain measured in vivo by ^{1}H magnetic resonance spectroscopy

João M.N. Duarte [a,b,*], Kim Q. Do [c], Rolf Gruetter [a,b,d]

[a] Laboratory for Functional and Metabolic Imaging, École Polytechnique Fédérale de Lausanne, Lausanne, Switzerland
[b] Department of Radiology, University of Lausanne, Lausanne, Switzerland
[c] Department of Psychiatry, Center for Psychiatric Neuroscience, Lausanne University Hospital, Lausanne, Switzerland
[d] Department of Radiology, University of Geneva, Geneva, Switzerland

ARTICLE INFO

Article history:
Received 24 May 2013
Received in revised form 19 November 2013
Accepted 27 January 2014
Available online 31 January 2014

Keywords:
Aging
Neurochemical profile
Biomarkers
^{1}H MRS
Brain
Metabolism

ABSTRACT

Alterations to brain homeostasis during development are reflected in the neurochemical profile determined noninvasively by ^{1}H magnetic resonance spectroscopy. We determined longitudinal biochemical modifications in the cortex, hippocampus, and striatum of C57BL/6 mice aged between 3 and 24 months . The regional neurochemical profile evolution indicated that aging induces general modifications of neurotransmission processes (reduced GABA and glutamate), primary energy metabolism (altered glucose, alanine, and lactate) and turnover of lipid membranes (modification of choline-containing compounds and phosphorylethanolamine), which are all probably involved in the frequently observed age-related cognitive decline. Interestingly, the neurochemical profile was different in male and female mice, particularly in the levels of taurine that may be under the control of estrogen receptors. These neurochemical profiles constitute the basal concentrations in cortex, hippocampus, and striatum of healthy aging male and female mice.

1. Introduction

Aging is accompanied by various cellular challenges in the brain, which lead to homeostatic alterations and ultimately result in the reduction of neuronal function and cognitive performance (Bizon et al., 2012). Although aging mechanisms are not fully understood, age-dependent brain modifications are likely reflected in alterations of the regional distribution of levels of neurochemicals. The concentration patterns of these compounds composing the neurochemical profile vary with cellular composition and function of the tissue, thus reflecting the structural differentiation of cerebral networks in a region-specific manner, and are affected by modification of functional states and by neuropathologies (reviewed in Duarte et al., 2012a). This supports the use of the neurochemical profile as region- and time-specific biomarker and, indeed, its noninvasive detection by magnetic resonance spectroscopy (MRS) has emerged as an important research tool in translational neuroscience. Neurochemical profiling has thus been successfully used to reliably probe brain biochemical modifications upon disease and/or treatment monitoring in mice (Berthet et al., 2011; Duarte et al., 2012b; Zacharoff et al. 2012), rats (Duarte et al., 2009; Rao et al., 2011), or humans (Bustillo et al., 2009; Seaquist et al., 2005). Each neuropathology has different etiology, is region specific and occurs with most prominence at a particular age range. For example, while schizophrenia is a neurodevelopment disorder, other nowadays-common disorders like Alzheimer's disease or Parkinson's disease mostly affect the middle aged and rapidly increasing elderly population. In humans, studies in elderly subjects were performed at low-magnetic field and focused on the most prominent resonances in ^{1}H nuclear magnetic resonance (NMR) spectra rather than determining an extensive neurochemical profile (Chang et al., 1996; Gruber et al., 2008; Schuff et al., 1999, 2001). In experimental animal models, the extended neurochemical profile detected in vivo by high-field ^{1}H MRS has been studied from birth to adulthood, disregarding the aging brain. Contributing for this is the fact that genetic manipulations in rodents allow to reach disease phenotypes at early age. Therefore, age-dependent modifications to the neurochemical profile remain to be investigated.

Most magnetic resonance scanners available for clinical routine are operating at low-magnetic field. Therefore, the extensive neurochemical profile observed in animal studies is not directly applicable to the clinical environment. Nevertheless, even at 1.5 T, several metabolites are distinguishable in ^{1}H MRS at short echo time (discussed in Duarte et al., 2012a). Then, analysis with appropriate algorithms provides measurements of several compounds such as

* Corresponding author at: Laboratory for Functional and Metabolic Imaging, École Polytechnique Fédérale de Lausanne, Station 6 (Bâtiment CH), CH-1015 Lausanne, Switzerland. Tel.: +41216937681.
E-mail address: joao.duarte@epfl.ch (J.M.N. Duarte).

0197-4580/$ – see front matter © 2014 Elsevier Inc. All rights reserved.
http://dx.doi.org/10.1016/j.neurobiolaging.2014.01.135

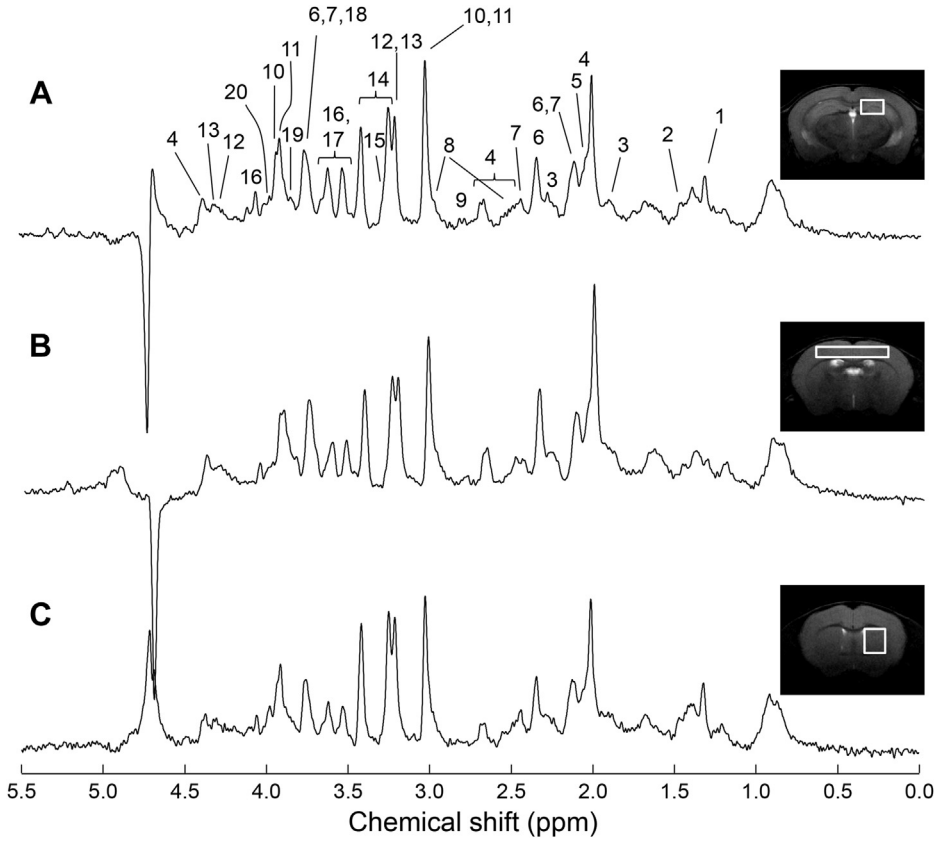

Fig. 1. Localized ^{1}H NMR spectra from the hippocampus (A), cortex (B) and striatum (C) of a 2-year-old female mouse acquired with SPECIAL at 14.1 T. Spectra were processed with Gaussian multiplication (gf = 0.08, gfs = 0.02), Fourier transformation and phase correction. Residual water signal removal or baseline correction was not applied. On the right of each spectrum, a representative fast-spin-echo image was used to show typical location of the volume of interest for spectroscopy. Metabolites in the spectra are assigned as follows: lactate (1), alanine (2), γ-aminobutyrate or GABA (3), *N*-acetylaspartate (4), *N*-acetylaspartylglutamate (5), glutamate (6), glutamine (7), glutathione (8), aspartate (9), phosphocreatine (10), creatine (11), phosphorylcholine (12), glycerylphosphorylcholine (13), taurine (14), *scyllo*-inositol (15), *myo*-inositol (16), glycine (17), ascorbate (18), glucose (19), phosphorylethanolamine (20).

creatine, *N*-acetylaspartate (NAA), *myo*-inositol, choline-containing compounds, and glutamate plus glutamine (the so called "Glx"). In a clinical 3.0 T system, Mekle et al. (2009) achieved spectral resolution sufficient to quantify a neurochemical profile composed 14 metabolites. The same neurochemical profile was determined with only 3 minutes of scan time at 7.0 T (Gambarota et al., 2009; Mekle et al., 2009; Tkáč et al., 2009) and at 9.4 T (Deelchand et al., 2010). This means that, at high field, the variety of neurochemicals detected in the human brain increasingly resemble those in rodents, that is, 20 metabolites. MRS is therefore a reliable method for diagnosing neurologic disorders and monitoring therapy outcomes, allowing early disease detection and preventive approaches. Furthermore, because the exact same tool can be applied noninvasively to rodents, high-field ^{1}H MRS in animal models with specific neuropathological phenotypes became a method of choice for translational research aiming at understanding biochemical mechanisms of disease development and progression. The aim of this study was to investigate the longitudinal modification of the neurochemical profile in vivo in the cortex, hippocampus, and striatum of C57BL/6 mice by ^{1}H MRS at 14.1 T. The analysis of these 3 brain areas aimed at depicting a diversity of brain functions and targets of neurologic disorders.

2. Methods

2.1. Animals

All experiments were conducted under approval of the local ethics committee in C57BL/6 mice that were born in the local animal facility. Mice were housed on a 12-hour light-dark cycle with room temperature at 22 °C and humidity at 50%–60%. Regular chow and tap water were provided ad libitum. The neurochemical profiles of hippocampus, cortex, and striatum were determined longitudinally in 36 mice (19 males and 17 females) at the age of 3, 6, 12, 18, and 24 months. All scans were performed during the light-cycle under anesthesia of 1%–1.5% isoflurane in oxygen gas and the duration of each NMR scanning session was restricted to a maximum of 120 minutes (Kulak et al., 2010).

2.2. MRS

Mice were fixed in a mouse holder with a bite bar and 2 ear inserts (RAPID Biomedical GmbH, Rimpar, Germany). Body temperature was maintained at 37 °C by warm water circulation. All experiments were carried out in a horizontal 14.1 T/26 cm magnet (Magnex Scientific, Abingdon, UK), with a 12 cm inner-diameter gradient (400 mT/m in 200 ms, minimized eddy currents), interfaced with a DirectDrive console (Agilent Technologies, Palo Alto, CA, USA). Radio frequency transmission and reception was achieved with a home-built quadrature surface coil composed of 2 geometrically decoupled single-turn loops of 12 mm inner diameter resonating at 600 MHz. The mouse brain was positioned in the isocenter of the magnet and located with fast-spin-echo images with repetition time of 4 seconds, echo time of 52 ms, and echo train length of 8. Field homogeneity in the region of interest was achieved with FAST(EST)MAP (Gruetter, 1993; Gruetter and Tkáč, 2000). Volumes of interest were placed in the hippocampus

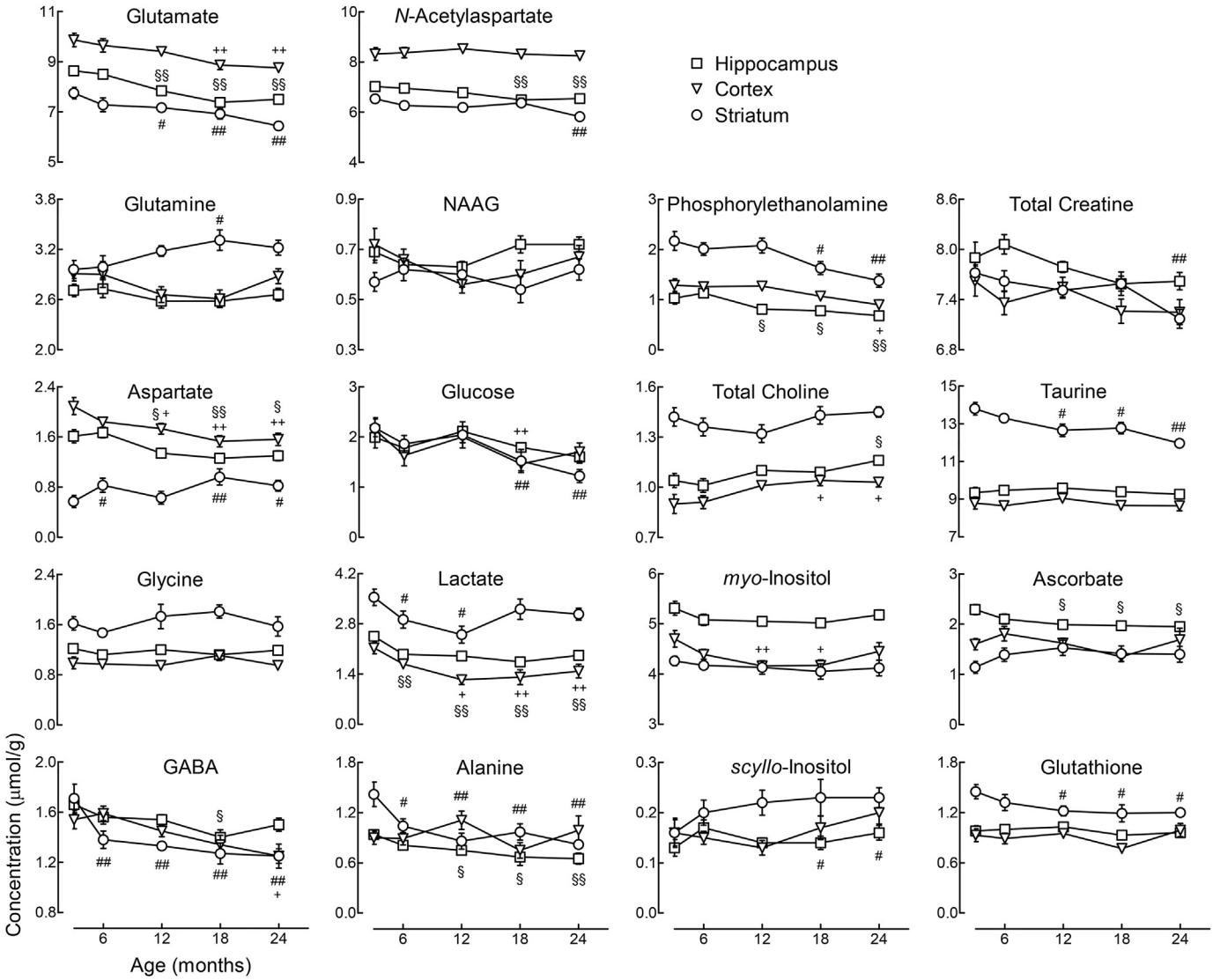

Fig. 2. Age-dependent modification of concentration of compounds that compose the neurochemical profile in the cortex (triangles), striatum (circles), and hippocampus (squares) of C57BL/6 mice. Neurochemical modifications were measured from ^{1}H NMR spectra acquired in vivo longitudinally from the 3 regions of the mouse brain aged 3, 6, 12, 18, and 24-month-old. §, +, and # represent significant differences at $p < 0.01$ compared with 3 months for the hippocampus, cortex, and striatum, respectively. Double symbols depict $p < 0.001$.

(1.3 × 1.9 × 1.8 mm^3), cortex (0.8 × 4.2 × 1.6 mm^3), or striatum (2.0 × 1.8 × 2.0 mm^3) of the C57BL/6 mice. NMR spectra were acquired using SPECIAL (Mlynárik et al., 2006) with echo time of 2.8 ms, repetition time of 4 seconds, and typically with 320–400 scans.

Metabolite concentrations were determined using the linear combination analysis method LCModel (Stephen Provencher Inc, Oakville, Ontario, Canada), including a macromolecule (Mac) spectrum in the database (Mlynárik et al., 2006; Duarte et al., 2012b). The unsuppressed water signal measured from the same volumes of interest was used as an internal reference for the absolute quantification of metabolites. The following 20 metabolites were included in the LCModel analysis: alanine (Ala), ascorbate (Asc), aspartate (Asp), creatine (Cre), γ-aminobutyrate (GABA), glutamine (Gln), glutamate (Glu), glutathione (GSH), glycine (Gly), glycerophosphorylcholine (GPC), glucose (Glc), lactate (Lac), *myo*-inositol (Ins), *N*-acetylaspartate (NAA), *N*-acetylaspartylglutamate (NAAG), phosphorylethanolamine (PE), phosphorylcholine (PCho), phosphocreatine (PCre), *scyllo*-inositol (scyllo), and taurine (Tau). The Cramér–Rao lower bound (CRLB) was provided by the LCModel as a measure of the reliability of the apparent metabolite concentration quantification. In most measured spectra, the present analysis was not able to reliably discern phosphorylcholine from glycerophosphorylcholine. Therefore, their sum was quantified as total choline-containing compounds (GPC + PCho or tCho). Because the relative content of creatine (Cre) and phosphocreatine (PCre) may depend on the energy status of the tissue, the total creatine concentration (Cre + PCre or tCre) was reported as a constitutive metabolic pool of the tissue. The ratios of PCre to Cre, Gln to Glu, and Asp to Glu were also analyzed.

2.3. Water content

Tissue water content was used for absolute quantification of neurochemicals. Thus, in another set of mice, water content variations during aging were determined in the cortex, hippocampus, and striatum at the age of 6, 12, and 24 months by the difference in wet and dry tissue weights. After decapitation under isoflurane

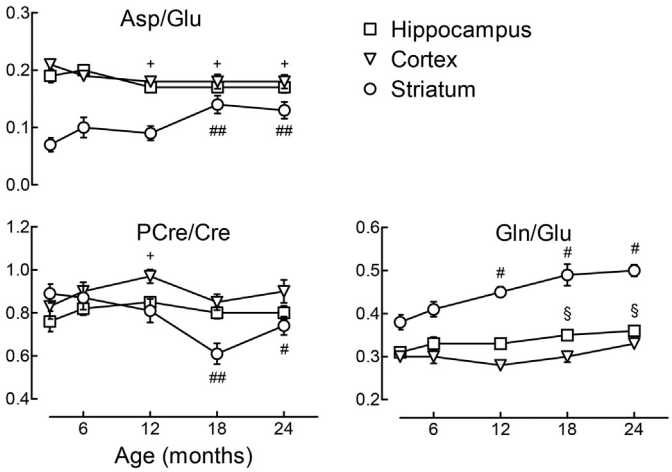

Fig. 3. Relevant metabolite ratios are modified upon aging in the mouse brain. Hippocampus, cortex, and striatum are represented by squares, triangles, and circles, respectively; §, +, and # represent significant differences at $p < 0.01$ compared with mice aged 3 months for the hippocampus, cortex, and striatum, respectively. Double symbols depict $p < 0.001$.

anesthesia, brain tissue was collected, weighed, and let to dry at 65 °C until dry weight did not vary. After desiccation, water content was calculated from the wet-dry weight difference. For younger animals, water content measurements were available from previous reports (Agrawal et al., 1968; Cohadon and Desbordes, 1986; Kulak et al., 2010; Larvaron et al., 2006).

2.4. Statistical analysis

Results are presented as mean ± standard error of the mean. Data were analyzed in IBM SPSS 20 (IBM Corp, Armonk, NY, USA) with multivariate analysis of variance (MANOVA), performed with respect to metabolite in the neurochemical profile, brain region and mouse gender, having age as a repeated factor. Then, metabolite-specific age effects with confidence level above 90% ($p < 0.1$) were followed up with paired t tests, for which significance level was set at $p < 0.01$. Correlation between quantified metabolites was tested with the Pearson correlation analysis to all measured datasets, that is, including 3 brain regions, 5 ages, and both genders.

3. Results

3.1. Quantification of neurochemicals

Typical ^{1}H NMR spectra from the rat brain in vivo exhibited excellent metabolite line widths (Fig. 1). In particular, for spectra acquired in the hippocampus, cortex, and striatum, respectively, average line width at half maximum was 16.1 ± 0.4 Hz, 19.7 ± 0.6 Hz, and 16.3 ± 0.5 Hz, as estimated by the LCModel. Water was consistently well suppressed and signal to noise was 21.0 ± 0.5, 18.4 ± 0.4, and 16.3 ± 0.3 in spectra from the hippocampus, cortex and striatum. This allowed determining a neurochemical profile of 19 metabolites that were quantified with CRLB generally below 25%. CRLB for glucose and phosphorylethanolamine were below 30% and for *scyllo*-inositol were lower than 40%.

In this study, water content was quantified by desiccation for the hippocampus, cortex, and striatum and used to determine absolute metabolite concentrations. Water fraction did not differ within experimental accuracy between the 3 measured regions of the mouse brain, but was substantially reduced with aging. At the age of 6 and 12 months, water content was 79 ± 1% (n = 4) and 79 ± 1% (n = 6), respectively, and reduced to 75 ± 1% at the age of 24 months (n = 9, $p < 0.01$ vs. 6 and 12 months). Average reported water content at the age of 1 month was 80 ± 1% (Agrawal et al., 1968; Cohadon and Desbordes, 1986; Kulak et al., 2010; Larvaron et al., 2006). Water content at these ages and interpolated at the age of 3 and 18 months was used to estimate absolute concentration of metabolites in the brain.

3.2. Regional variation of metabolite concentrations

Regional specificity of spectral lines was directly evident from the relative height of NAA, creatine, and taurine peaks in ^{1}H NMR spectra acquired in vivo in the cortex, striatum, and hippocampus of adult mice (Fig. 1). The concentration of metabolites in the neurochemical profile across the brain regions varied between the age of 3 and 24 months (Fig. 2). Analysis of these results with MANOVA clearly indicated that the neurochemical profile is region specific (Supplementary Table 1). Although only glucose was not statistically different in the 3 brain regions ($F = 1.431$, $p > 0.05$), the age evolution of metabolite concentrations was generally similar, except for taurine, NAAG, and glycine that displayed significant region-age or region-age-gender interactions (Supplementary Table 1).

3.3. Aging-dependent neurochemical modifications

The most prominent age-dependent neurochemical modifications were in the concentration of metabolites involved in neurotransmission, energy metabolism, or maintenance of cellular membranes (Fig. 2, Supplementary Tables 1 and 2). In particular, the main excitatory and inhibitory neurotransmitters, glutamate and GABA, were substantially reduced upon aging in the measured regions ($p < 0.001$). Compared with young adult mice, that is, at the age of 3 months, glutamate was reduced in the hippocampus, cortex, and striatum of 2-year-old mice by 13 ± 1%, 11 ± 2%, and 17 ± 2% ($p < 0.001$) and GABA was decreased by 10 ± 3%, 19 ± 6%, and 27 ± 3% ($p < 0.001$), respectively. Aspartate was also reduced ($p < 0.05$) in the cortex (−25 ± 5%, 24 vs. 3 months) and hippocampus (−19 ± 5%, 24 vs. 3 months) but not in striatum (+44 ± 15%, 24 vs. 3 months).

This modification in levels of neuroactive-amino acids was accompanied by a reduction in the concentration of glucose ($p < 0.01$, 24 vs. 3 months: −19.6 ± 6.3%, −20.6 ± 8.4%, and −44.0 ± 5.9% in the hippocampus, cortex, and striatum, respectively), as well as in lactate ($p < 0.001$) and/or alanine ($p < 0.001$).

Compounds involved in lipid metabolism and plasma membrane turnover were modified in the 3 measured regions. Namely, while aging was associated with a reduction in the concentration of phosphorylethanolamine in the hippocampus, cortex, and striatum ($p < 0.001$; −34 ± 5%, −30 ± 7%, and −36 ± 6% for 24 vs. 3 months, respectively), choline-containing compounds increased over the 2 years ($p < 0.01$; 24 vs. 3 months: +12 ± 2%, +14 ± 3%, and +2 ± 2% in the hippocampus, cortex, and striatum, respectively).

The content of *myo*-inositol was reduced after the age of 3 months and displayed a tendency to increase in brain regions of 2-year-old mice ($p < 0.01$), while the other isomer of inositol present in the brain in important amounts, *scyllo*-inositol, increased with age ($p < 0.05$). Total creatine, which is frequently taken as a reference compound in MRS studies, was found to decrease with age in the hippocampus, cortex, and striatum by −4 ± 1%, −5 ± 2%, and −7 ± 2%, respectively (24 vs. 3 months, $p < 0.05$). In adult mice, taurine concentration only varied with age in the striatum (−13 ± 4% for 24 vs. 3 months, $p < 0.05$). Glutathione showed an evolving pattern similar to that of taurine, being modified in the striatum

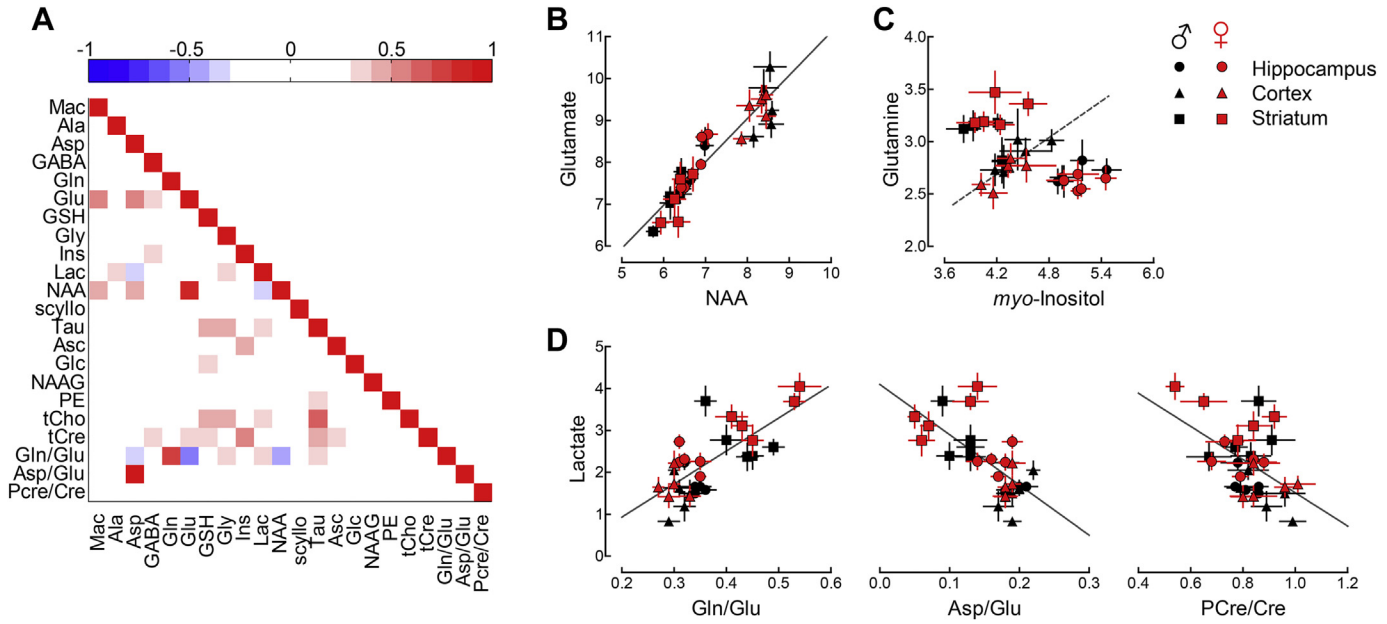

Fig. 4. Correlation between metabolite concentrations and/or ratios that are putative markers of specific cell populations and metabolic states. (A) Pearson correlation coefficients (r) depict linear dependence between metabolite concentrations and/or metabolite ratios within the measured neurochemical profile. (B) Demonstrates the correlation of regional glutamate and NAA concentrations across mouse age and gender. The resulting slope in linear fit is represented by the gray line ($R^2 = 0.859$). (C) Glutamine versus *myo*-inositol concentrations. Dashed line represents the linear relation between glutamine and *myo*-inositol in data from the cortex ($R^2 = 0.659$). (D) Relation between lactate concentration and metabolite ratios Gln to Glu ($R^2 = 0.524$), Asp to Glu ($R^2 = 0.472$), and PCre to Cre ($R^2 = 0.263$). (B–D) Data from hippocampus, striatum, and cortex are shown in circles, squares and triangles, respectively. Data from female mice are colored in red, while black depicts male mice. *Abbreviation: NAA, N-acetylaspartate.*

(−17 ± 4% for 24 vs. 3 months, $p < 0.01$), but not in the other measured regions.

Important metabolite ratios were determined and also displayed regional specific and/or age-dependent modification: Gln to Glu, Asp to Glu, PCre to Cre (Fig. 3). Most prominently, Gln to Glu increased with age in the hippocampus, cortex, and striatum by +16 ± 4%, +10 ± 3%, and +32 ± 4%, respectively (24 vs. 3 months, $p < 0.05$).

3.4. Correlation between neurochemicals

Pearson correlation coefficients (r) were calculated to find probable linear dependences between measured metabolites and/or metabolite ratios. As depicted in Fig. 4A, besides the obvious correlation of metabolites and their calculated concentration ratios, many compounds of the neurochemical profile were significantly correlated. The strongest correlation was found between the two putative neuronal markers NAA and glutamate ($r = 0.821$, $p < 0.01$; plot in Fig. 4B). Linear fit of glutamate to NAA concentrations across the brain region, age, and mouse gender, resulted in a significant slope of 1.0 ± 0.1 ($F = 170.9$, $p < 0.0001$) and y-intercept of 0.8 ± 0.6 μmol/g ($R^2 = 0.859$). While the putative glial marker *myo*-inositol and glutamine that is specifically produced in glial cells by glutamine synthetase did not generally correlate ($r = -0.034$, $p > 0.05$), a linear relation between glutamine and myo-inositol was specifically detected in the cortex ($R^2 = 0.659$; slope of 0.58 ± 0.15 with $F = 15.47$, $p < 0.01$; y-intercept of 0.25 ± 0.65 μmol/g, Fig. 4C). Among other significant correlations throughout all regions (Fig. 4A), we found: taurine and choline-containing compounds ($r = 0.633$, $p < 0.01$), *myo*-inositol and total creatine ($r = 0.519$, $p < 0.01$), glutamate and aspartate ($r = 0.558$, $p < 0.01$). Interestingly, less strong but significant correlations were found between lactate and physiologically important metabolite ratios (Fig. 4D), namely Gln to Glu ($r = 0.311$, $p < 0.01$), Asp to Glu ($r = -0.261$, $p < 0.01$), and PCre to Cre ($r = -0.251$, $p < 0.01$). Linear relations between lactate concentration and these metabolite ratios were as follows: Gln to Glu with slope 7.9 ± 1.4 μmol/g ($F = 30.87$, $p < 0.001$) and y = −0.64 ± 0.52 μmol/g at x = 0 ($R^2 = 0.524$); Asp to Glu with slope −12.0 ± 2.4 μmol/g ($F = 24.98$, $p < 0.001$) and y = 4.1 ± 0.4 μmol/g at x = 0 of ($R^2 = 0.472$); PCre to Cre with slope −4.0 ± 1.3 μmol/g ($F = 10.01$, $p < 0.01$) and y = 5.5 ± 1.0 μmol/g at x = 0 of ($R^2 = 0.263$).

3.5. Gender differences

The evolution of the neurochemical profile with age was dependent on gender, most importantly in taurine, ascorbate, and total creatine content ($p < 0.001$, Fig. 5A). A gender effect was also found for the evolution of glucose ($p < 0.05$), lactate and alanine ($p < 0.01$ for both), as well as for phosphorylethanolamine ($p < 0.01$) and aspartate ($p < 0.05$). Interestingly, because taurine is a substantially concentrated metabolite in the mouse brain, reaching concentrations that range between 7 and 15 μmol/g, the simple combination of taurine content with levels of NAA and *myo*-inositol, allowed to directly separate neurochemical profiles by both scanned brain region and mouse gender (Fig. 5B).

4. Discussion

The present study reports, for the first time, longitudinal neurochemical modifications in the cortex, hippocampus, and striatum of the aging mouse, measured noninvasively by high-field ^{1}H MRS. The most prominent modifications were in metabolites involved in the processes of neurotransmission, energy production, and membrane lipid metabolism.

Neurotransmitters such as glutamate and GABA decreased during aging, suggesting reduction of synaptic function. In line with this, age-dependent reduction in the density of synaptic proteins were reported in the rodent brain, namely SNARE complex proteins,

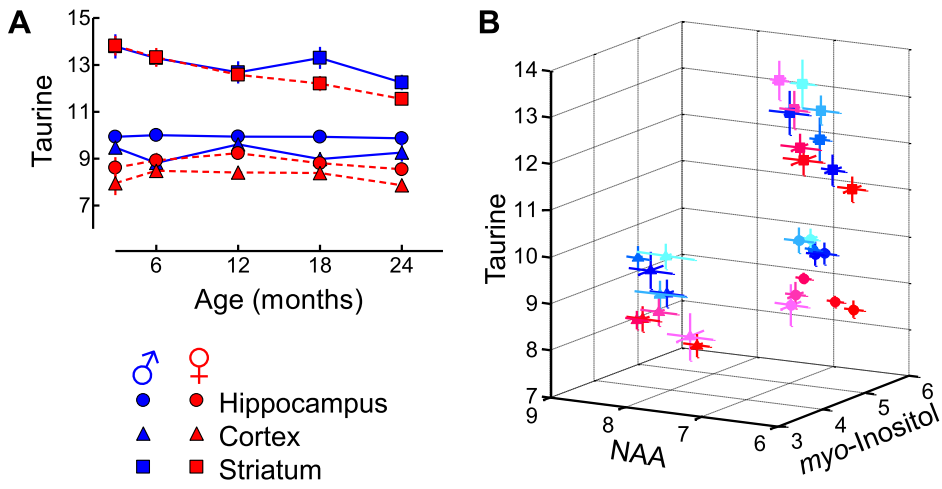

Fig. 5. Three metabolites that occur at relatively high levels in the mouse brain allow differentiating both brain region and mouse gender. (A) Taurine concentration in the cortex and hippocampus allows distinguishing the mice gender. Indeed, the simultaneous plot of taurine against 2 putative cell-specific markers, NAA for neurons and *myo*-inositol for glia, clearly separates the data in measured region and mouse gender (B). Data from the hippocampus, striatum, and cortex are shown in circles, squares, and triangles, respectively. Data from male and female mice are shown in blue and red, respectively. (B) Darker colors represent older mice.

vesicle-mobilizing proteins, vesicular neurotransmitter transporters, postsynaptic proteins, and components of the synaptic vesicle cycle (Canas et al., 2009; VanGuilder et al., 2010), which can contribute to the hippocampal function decline and thus to reduction of memory performance (Allard et al., 2012; Gage et al., 1984a; Kennard and Woodruff-Pak, 2011; Pistell et al., 2012).

Because glutamine is exclusively synthesized in glial cells mostly from synaptic-born glutamate, and then shuttled back to replenish glutamate neurotransmitter pools in neurons, Gln/Glu may reflect glutamate-glutamine cycle activity between neurons and glial cells. In line with this, the aging-associated reduction of synaptic connectivity was accompanied by Gln/Glu increase in the cortex, striatum, and hippocampus. For a long time, noninvasive detection of a peak corresponding mainly to resonances of both glutamate and glutamine in the cerebral tissue has been taken as a marker of function and degeneration in the preclinical and clinical studies. An independent noninvasive measure of both and also their ratio at high-magnetic field strength may provide a more specific marker to indicate neuronal function and dysfunction (as glutamate and glutamine are mostly located in neurons and glia, respectively). For example, impaired neurotransmission and excitotoxicity after an ischemic insult lead to transient glutamate decrease and glutamine accumulation (Berthet et al., 2011; Lei et al., 2009). In line with this idea, disturbed glutamatergic neurotransmission in schizophrenia leads to altered levels of glutamine, glutamate, and most notably of Gln/Glu, as observed in translational and clinical ^{1}H MRS studies (Bustillo et al., 2009; Duarte et al., 2012b; Hashimoto et al., 2005; Lutkenhoff et al., 2008; Shirayama et al., 2010; Tayoshi et al., 2009).

In the healthy mouse brain, we observed a tendency ($p = 0.076$) for loss of NAA in the hippocampus and striatum with aging but not in the cortex, where its concentration was the highest (Fig. 2). NAA is mainly produced and stored in neurons and shuttled to oligodendrocytes for myelin production, and it has been used as a marker of neuronal function or density (reviewed in Duarte et al., 2012a). Similarly, glutamate mainly resides in neurons, being readily converted to glutamine in glial cells (Gruetter et al., 2003; McKenna, 2007 and references therein). Accordingly, the results in Fig. 4 show good correlation between the levels of NAA and glutamate in the mouse brain in vivo.

In contrast, increased levels of *myo*-inositol have been taken as marker of astrogliosis and, in fact, in Alzheimer's disease, while NAA loss is frequently associated with neuronal degeneration, increased levels of *myo*-inositol are often related to other specific markers of astrocyte reactivity (discussed in Duarte et al., 2012a). This is however debatable and some studies failed to find a correlation between pathology-associated astrogliosis and *myo*-inositol levels (Duarte et al., 2009; Kim et al., 2005; Kunz et al., 2011). In addition, glutamine synthetase is specific to glial cells and we found a linear relation between *myo*-inositol and glutamine concentrations only in the cortex, suggesting that *myo*-inositol cannot be taken as a general marker of astrogliosis (Fig. 4C).

The age-dependent modifications now observed in the mouse brain resemble those in humans. For example, an elegant study by Boumezbeur et al., (2010) found a reduction in NAA (−10%) and glutamate (−14%) and increase in *myo*-inositol (+25%) concentrations in the brain of elderly humans, compared with young subjects, which could result in higher Gln/Glu (Fig. 3). In addition, neuronal and glial mitochondrial metabolism and glutamate-glutamine cycle flux was lower in elderly subjects (Boumezbeur et al., 2010).

Glucose transport and consumption vary between brain regions and they result in lower glucose content in the striatum, compared with the hippocampus and cortex (reviewed in Barros et al., 2007). Although regional variation of glucose levels was not found because isoflurane anesthesia alters glucose homeostasis (Duarte and Gruetter, 2012b), lactate that results from glycolytic metabolism had distinct levels in the cortex, striatum, and hippocampus. Furthermore, lactate levels decreased with age, which is in accordance with reduced cerebral glucose utilization upon aging (Gage et al., 1984b; Tack et al., 1989). This difference in lactate content may be indicative of the relative rates of cytosolic glycolysis and mitochondrial oxidative metabolism, further supported by putative differences in PCre/Cre, which is indicative of adenosine 5′-triphosphate (ATP) buffering by creatine kinase, and Asp/Glu, which may indicate integrity of the malate-aspartate shuttle in mitochondria. Aspartate and glutamate are essential for the transport of reducing equivalents from cytosol into mitochondria through the malate-aspartate shuttle to be oxidized in the electron chain and produce ATP. Asp/Glu was not significantly altered by aging but demonstrates regional differences, that is, it was lower in the striatum compared with the other regions. This suggests differences in cytosolic production of reducing equivalents produced in glycolysis that are then transferred into the mitochondrial matrix through the malate-

aspartate shuttle, a major step in neuroenergetics (Gruetter et al., 2003; McKenna, 2007). Therefore, measurement of these 2 amino acids may link excitatory neurotransmission to energy production and consumption (Duarte et al., 2012a; Kunz et al., 2011).

Lactate levels correlated with Gln/Glu, suggesting that glutamine accumulation in astrocytes, possibly because of increased glutamate-glutamine cycling, was associated with an increased rate of glycolysis relative to that of mitochondrial oxidative metabolism, in accordance to the increased glucose consumption rate with brain activity (discussed in Duarte and Gruetter, 2012a, 2012b). In line with this, increased brain activity leads to ammonia accumulation that requires detoxification through glutamine synthesis (discussed in Merle and Franconi, 2012). A positive association of lactate concentration with Gln/Glu is in agreement with the proposed coupling of glial glycolysis and excitatory glutamatergic neurotransmission (Pellerin and Magistretti, 2012). In addition, concentration of brain lactate was inversely associated to PCre/Cre and Asp/Glu, which is explained by higher rate of glycolysis when there is less storage of high energy phosphates by the buffer system operated by creatine kinase, that is, less abundance of ATP, and consequent increased rate of the aspartate aminotransferase that is essential for the malate-aspartate shuttle.

Compounds involved in membrane metabolism were modified with age. In particular, phosphorylethanolamine content was reduced while tCho increased. Because in the brain choline is below the NMR detection limit and mainly GPC and PCho contribute to this intense resonance, the measured choline-containing compounds are likely reflecting membrane lipid synthesis rather than the biosynthesis of the neurotransmitter acetylcholine (reviewed in Duarte et al., 2012a). During early development, brain choline increases with age in the mouse cortex (Kulak et al., 2010). The present study shows that this increase of tCho with age continued through adulthood and aging and that this increase was not specific to the cortex. As reviewed in Duarte et al. (2012a), total choline concentration in the human brain is positively correlated with age, which has been attributed to increased release of water-soluble choline-containing compounds from cell membranes, reflecting higher membrane turnover. Phosphorylethanolamine is a precursor for phosphatidylethanolamine, which is a major phospholipid in the brain, and its concentration decreases during cerebral development in both rodents and humans, paralleling the decrease of myelination and cellular proliferation (Duarte et al., 2012a). Like tCho, phosphorylethanolamine levels continued their developmental trend for decrease during adulthood and aging. The inverse trajectory in the evolution of tCho and phosphorylethanolamine levels in the aging brain may be related to modifications in cell membrane fluidity (Calderini et al., 1983). In line with this, a ^{31}P MRS study showed that the glycerylated forms of such phospholipids increase with age in the human brain (Blüml et al., 1999).

Frequently, total creatine is used as a reference for the remaining metabolite concentrations. However, its concentration (signal) was found to change in certain pathologic conditions (Duarte et al., 2012b, 2009), during postnatal development (Kulak et al., 2010) and between gray and white matter (Mukherjee et al., 2000). Reduction of total creatine concentration with age was observed in the cortex, hippocampus, and striatum during aging (Fig. 2), suggesting that care should be taken when using creatine as a normalization factor.

Our previous study on neurochemical modifications during early development in the mouse cortex demonstrated a marked reduction in taurine levels from the age of 10 days to 3 months (Kulak et al., 2010). Taurine content was not modified with aging in the hippocampus or cortex in adult mice. In contrast, it continuously decreased during aging in the striatum, where it is most concentrated. Among other functions, taurine is also a neuromodulator and interacts with inhibitory $GABA_A$, $GABA_B$, or glycine receptors thus, displaying capability of modulating synaptic plasticity (reviewed in Albrecht and Schousboe, 2005). This inhibitory role of taurine is especially important during the period of cortical synaptogenesis, when brain taurine levels are found to be the highest (Kulak et al., 2010; Tkáč et al., 2003). However, as a small fraction of taurine is involved in neuromodulation (particularly in the case of rodents), the main role of taurine may be rather related to osmoregulation, balancing modifications in glutamate, glutamine, NAA, and other major neurochemicals during development (Kulak et al., 2010).

This study was performed in both male and female mice and the neurochemical profile was similar in both genders. Nevertheless, some neurochemical differences between genders were identified by MANOVA. In particular, taurine concentration that was consistently lower in the cortex and hippocampus of female mice, relative to age-matched males. In the striatum, this gender-associated difference in taurine levels was only present in aged mice. Thus, taurine concentration seems to be related to estrogen activity in the brain. Indeed, estrogen receptors regulate taurine uptake via the Na^+-dependent taurine transporter (TauT) in MCF-7 human breast cancer cells (Han et al., 2006; Shennan and Thomson, 2007). Both estrogen receptors ERα and ERβ are present in the mouse cortex, hippocampus, and striatum, although striatal levels of either messenger RNA or protein are much lower (Küppers and Beyer, 1999; Mitra et al., 2003; Shughrue and Merchenthaler, 2000). Estrogen receptors modulate brain function and, like taurine, afford neuroprotection in the cortex and hippocampus (Shughrue and Merchenthaler, 2000). Although the striatum is not protected by estrogen after ischemic injury (Shughrue and Merchenthaler, 2000), estrogen receptors afford neuroprotection of striatal dopaminergic neurons in animal models of Parkinson's disease (Al Sweidi et al., 2012; Campos et al., 2012), possibly by regulating dopamine transport (Di Liberto et al., 2012) or microgliosis (Liu et al., 2005).

It should be noted that during early development of the mouse cortex from P10 to adult age (Kulak et al., 2010), most metabolite concentrations increased upon tissue differentiation, particularly glutamate, glutamine, aspartate, NAA, *myo*-inositol, creatine, and choline containing compounds. In the present study, while cortical glutamine and NAA levels were relatively stable (at a 3 and 8.5 μmol/g, respectively), tCho continued increasing, but glutamate, aspartate, and creatine concentrations decreased during adult age. Because the juvenile increase in brain metabolite concentrations appeared asymptotic toward adulthood (Kulak et al., 2010), different mechanisms must drive metabolic alterations upon aging. The underlying mechanisms for these alterations remain to be explored.

In conclusion, the neurochemical profile varies upon healthy aging in the mouse brain and suggests that aging is associated to modifications of energy metabolism, synaptic transmission, and cell membrane turnover. Furthermore, while NAA and glutamate may be relevant markers for neuronal density or function, myo-inositol does not appear to be a general marker for the glial compartment. This study provided the basal neurochemical profiles of the cortex, hippocampus, and striatum of healthy aging male and female mice. Because the neurochemical profile is specific for a given cerebral status and can also be measured in the human brain, it serves as a noninvasive biomarker for the detection of neurologic disorders and for therapy monitoring.

Disclosure statement

All authors disclose no conflicts of interest.

Acknowledgements

This work was supported by the Centre d'Imagerie BioMédicale of the UNIL, UNIGE, HUG, CHUV, EPFL, and the Leenaards and Jeantet Foundations, by the Swiss National Science Foundation (Grant 310030-135736 to Kim Q Do) and by the Loterie Romande.

Appendix A. Supplementary data

Supplementary data associated with this article can be found, in the online version, at http://dx.doi.org/10.1016/j.neurobiolaging.2014.01.135.

References

Agrawal, H.C., Davis, J.M., Himwich, W.A., 1968. Developmental changes in mouse brain: weight, water content and free amino acids. J. Neurochem. 15, 917–923.
Al Sweidi, S., Sánchez, M.G., Bourque, M., Morissette, M., Dluzen, D., Di Paolo, T., 2012. Oestrogen receptors and signalling pathways: implications for neuroprotective effects of sex steroids in Parkinson's disease. J. Neuroendocrinol. 24, 48–61.
Albrecht, J., Schousboe, A., 2005. Taurine interaction with neurotransmitter receptors in the CNS: an update. Neurochem. Res. 30, 1615–1621.
Allard, S., Scardochio, T., Cuello, A.C., Ribeiro-da-Silva, A., 2012. Correlation of cognitive performance and morphological changes in neocortical pyramidal neurons in aging. Neurobiol. Aging 33, 1466–1480.
Barros, L.F., Bittner, C.X., Loaiza, A., Porras, O.H., 2007. A quantitative overview of glucose dynamics in the gliovascular unit. Glia 55, 1222–1237.
Berthet, C., Lei, H., Gruetter, R., Hirt, L., 2011. Early predictive biomarkers for lesion after transient cerebral ischemia. Stroke 42, 799–805.
Bizon, J.L., Foster, T.C., Alexander, G.E., Glisky, E.L., 2012. Characterizing cognitive aging of working memory and executive function in animal models. Front. Ag. Neurosci. 4, 19.
Boumezbeur, F., Mason, G.F., de Graaf, R.A., Behar, K.L., Cline, G.W., Shulman, G.I., Rothman, D.L., Petersen, K.F., 2010. Altered brain mitochondrial metabolism in healthy aging as assessed by in vivo magnetic resonance spectroscopy. J. Cereb. Blood Flow. Metab. 30, 211–221.
Bustillo, J.R., Rowland, L.M., Mullins, P., Jung, R., Chen, H., Qualls, C., Hammond, R., Brooks, W.M., Lauriello, J., 2009. ^{1}H-MRS at 4 tesla in minimally treated early schizophrenia. Mol. Psychiatry 15, 629–636.
Blüml, S., Seymour, K.J., Ross, B.D., 1999. Developmental changes in choline- and ethanolamine-containing compounds measured with proton-decoupled 31P MRS in in vivo human brain. Magn. Reson. Med. 42, 643–654.
Calderini, G., Bonetti, A.C., Battistella, A., Crews, F.T., Toffano, G., 1983. Biochemical changes of rat brain membranes with aging. Neurochem. Res. 8, 483–492.
Campos, F.L., Cristovão, A.C., Rocha, S.M., Fonseca, C.P., Baltazar, G., 2012. GDNF contributes to oestrogen-mediated protection of midbrain dopaminergic neurones. J. Neuroendocrinol. 24, 1386–1397.
Canas, P.M., Duarte, J.M.N., Rodrigues, R.J., Köfalvi, A., Cunha, R.A., 2009. Modification upon aging of the density of presynaptic modulation systems in the hippocampus. Neurobiol. Aging 30, 1877–1884.
Chang, L., Ernst, T., Poland, R.E., Jenden, D.J., 1996. In vivo proton magnetic resonance spectroscopy of the normal aging human brain. Life Sci. 58, 2049–2056.
Cohadon, F., Desbordes, P., 1986. Brain water and aging. Gerontology 32 (Suppl 1), 46–49.
Deelchand, D.K., Van de Moortele, P.F., Adriany, G., Iltis, I., Andersen, P., Strupp, J.P., Vaughan, J.T., Uğurbil, K., Henry, P.G., 2010. In vivo ^{1}H NMR spectroscopy of the human brain at 9.4 T: initial results. J. Magn. Reson. 206, 74–80.
Di Liberto, V., Mäkelä, J., Korhonen, L., Olivieri, M., Tselykh, T., Mälkiä, A., Do Thi, H., Belluardo, N., Lindholm, D., Mudò, G., 2012. Involvement of estrogen receptors in the resveratrol-mediated increase in dopamine transporter in human dopaminergic neurons and in striatum of female mice. Neuropharmacology 62, 1011–1018.
Duarte, J.M.N., Carvalho, R.A., Cunha, R.A., Gruetter, R., 2009. Caffeine consumption attenuates neurochemical modifications in the hippocampus of streptozotocin-induced diabetic rats. J. Neurochem. 111, 368–379.
Duarte, J.M.N., Gruetter, R., 2012a. Cerebral glucose transport and homeostasis. In: Choi, I.-Y., Gruetter, R. (Eds.), Neural Metabolism In Vivo. Springer, New York, pp. 655–673.
Duarte, J.M.N., Gruetter, R., 2012b. Characterization of cerebral glucose dynamics in vivo with a four-state conformational model of transport at the blood-brain-barrier. J. Neurochem. 121, 396–406.
Duarte, J.M.N., Kulak, A., Gholam-Razaee, M.M., Cuenod, M.R., Gruetter, R., Do, K.Q., 2012b. N-acetylcysteine normalizes neurochemical changes in the glutathione-deficient schizophrenia mouse model during development. Biol. Psychiatry 71, 1006–1014.
Duarte, J.M.N., Lei, H., Mlynárik, V., Gruetter, R., 2012a. The neurochemical profile quantified by in vivo ^{1}H NMR spectroscopy. NeuroImage 61, 342–362.
Gage, F.H., Dunnett, S.B., Björklund, A., 1984a. Spatial learning and motor deficits in aged rats. Neurobiol. Aging 5, 43–48.
Gage, F.H., Kelly, P.A., Björklund, A., 1984b. Regional changes in brain glucose metabolism reflect cognitive impairments in aged rats. J. Neurosci. 4, 2856–2865.
Gambarota, G., Mekle, R., Xin, L., Hergt, M., van der Zwaag, W., Krueger, G., Gruetter, R., 2009. In vivo measurement of glycine with short echo-time ^{1}H MRS in human brain at 7 T. MAGMA 22, 1–4.
Gruber, S., Pinker, K., Riederer, F., Chmelík, M., Stadlbauer, A., Bittsanský, M., Mlynárik, V., Frey, R., Serles, W., Bodamer, O., Moser, E., 2008. Metabolic changes in the normal ageing brain: consistent findings from short and long echo time proton spectroscopy. Eur. J. Radiol. 68, 320–327.
Gruetter, R., 1993. Automatic, localized in vivo adjustment of all first- and second-order shim coils. Magn. Reson. Med. 29, 804–811.
Gruetter, R., Adriany, G., Choi, I.Y., Henry, P.G., Lei, H., Oz, G., 2003. Localized in vivo ^{13}C NMR spectroscopy of the brain. NMR Biomed. 16, 313–338.
Gruetter, R., Tkác, I., 2000. Field mapping without reference scan using asymmetric echo-planar techniques. Magn. Reson. Med. 43, 319–323.
Han, X., Patters, A.B., Jones, D.P., Zelikovic, I., Chesney, R.W., 2006. The taurine transporter: mechanisms of regulation. Acta Physiol. (Oxf) 187, 61–73.
Hashimoto, K., Engberg, G., Shimizu, E., Nordin, C., Lindström, L.H., Iyo, M., 2005. Elevated glutamine/glutamate ratio in cerebrospinal fluid of first episode and drug naive schizophrenic patients. BMC Psychiatry 5, 6.
Kennard, J.A., Woodruff-Pak, D.S., 2011. Age sensitivity of behavioral tests and brain substrates of normal aging in mice. Front. Aging Neurosci. 3, 9.
Kim, J.P., Lentz, M.R., Westmoreland, S.V., Greco, J.B., Ratai, E.M., Halpern, E., Lackner, A.A., Masliah, E., González, R.G., 2005. Relationships between astrogliosis and ^{1}H MR spectroscopic measures of brain choline/creatine and *myo*-inositol/creatine in a primate model. Am. J. Neuroradiol. 26, 752–759.
Kulak, A., Duarte, J.M.N., Do, K.Q., Gruetter, R., 2010. Neurochemical profile of the developing mouse cortex determined by in vivo ^{1}H NMR spectroscopy at 14.1 T and the effect of recurrent anaesthesia. J. Neurochem. 115, 1466–1477.
Kunz, N., Camm, E.J., Somm, E., Lodygensky, G., Darbre, S., Aubert, M.L., Hüppi, P.S., Sizonenko, S.V., Gruetter, R., 2011. Developmental and metabolic brain alterations in rats exposed to bisphenol A during gestation and lactation. Int. J. Dev. Neurosci. 29, 37–43.
Küppers, E., Beyer, C., 1999. Expression of estrogen receptor-alpha and beta mRNA in the developing and adult mouse striatum. Neurosci. Lett. 276, 95–98.
Larvaron, P., Bielicki, G., Boespflug-Tanguy, O., Renou, J.P., 2006. Proton MRS of early post-natal mouse brain modifications in vivo. NMR Biomed. 19, 180–187.
Lei, H., Berthet, C., Hirt, L., Gruetter, R., 2009. Evolution of the neurochemical profile after transient focal cerebral ischemia in the mouse brain. J. Cereb. Blood Flow. Metab. 29, 811–819.
Liu, X., Fan, X.L., Zhao, Y., Luo, G.R., Li, X.P., Li, R., Le, W.D., 2005. Estrogen provides neuroprotection against activated microglia-induced dopaminergic neuronal injury through both estrogen receptor-alpha and estrogen receptor-beta in microglia. J. Neurosci. Res. 81, 653–665.
Lutkenhoff, E.S., van Erp, T.G., Thomas, M.A., Therman, S., Manninen, M., Huttunen, M.O., Kapiro, J., Lönnqvist, J., O'Neill, J., Cannon, T.D., 2008. Proton MRS in twin pairs discordant for schizophrenia. Mol. Psychiatry 15, 308–318.
McKenna, M.C., 2007. The glutamate-glutamine cycle is not stoichiometric: fates of glutamate in brain. J. Neurosci. Res. 85, 3347–3358.
Mekle, R., Mlynárik, V., Gambarota, G., Hergt, M., Krueger, G., Gruetter, R., 2009. MR spectroscopy of the human brain with enhanced signal intensity at ultrashort echo times on a clinical platform at 3T and 7T. Magn. Reson. Med. 61, 1279–1285.
Merle, M., Franconi, J.-M., 2012. Brain metabolic compartmentalization, metabolism modeling, and cerebral activity-metabolism relationship. In: Choi, I.-Y., Gruetter, R. (Eds.), Neural Metabolism In Vivo. Springer, New York, pp. 947–992.
Mitra, S.W., Hoskin, E., Yudkovitz, J., Pear, L., Wilkinson, H.A., Hayashi, S., Pfaff, D.W., Ogawa, S., Rohrer, S.P., Schaeffer, J.M., McEwen, B.S., Alves, S.E., 2003. Immunolocalization of estrogen receptor beta in the mouse brain: comparison with estrogen receptor alpha. Endocrinology 144, 2055–2067.
Mlynárik, V., Gambarota, G., Frenkel, H., Gruetter, R., 2006. Localized short-echo-time proton MR spectroscopy with full signal-intensity acquisition. Magn. Reson. Med. 56, 965–970.
Mukherjee, P., Bahn, M.M., McKinstry, R.C., Shimony, J.S., Cull, T.S., Akbudak, E., Snyder, A.Z., Conturo, T.E., 2000. Differences between gray matter and white matter water diffusion in stroke: diffusion-tensor MR imaging in 12 patients. Radiology 215, 211–220.
Pellerin, L., Magistretti, P.J., 2012. Sweet sixteen for ANLS. J. Cereb. Blood Flow. Metab. 32, 1152–1166.
Pistell, P.J., Spangler, E.L., Kelly-Bell, B., Miller, M.G., de Cabo, R., Ingram, D.K., 2012. Age-associated learning and memory deficits in two mouse versions of the stone T-maze. Neurobiol. Aging 33, 2431–2439.
Rao, R., Tkáč, I., Schmidt, A.T., Georgieff, M.K., 2011. Fetal and neonatal iron deficiency causes volume loss and alters the neurochemical profile of the adult rat hippocampus. Nutr. Neurosci. 14, 59–65.
Schuff, N., Amend, D.L., Knowlton, R., Norman, D., Fein, G., Weiner, M.W., 1999. Age-related metabolite changes and volume loss in the hippocampus by magnetic resonance spectroscopy and imaging. Neurobiol. Aging 20, 279–285.
Schuff, N., Ezekiel, F., Gamst, A.C., Amend, D.L., Capizzano, A.A., Maudsley, A.A., Weiner, M.W., 2001. Region and tissue differences of metabolites in normally aged brain using multislice ^{1}H magnetic resonance spectroscopic imaging. Magn. Reson. Med. 45, 899–907.
Seaquist, E.R., Tkáč, I., Damberg, G., Thomas, W., Gruetter, R., 2005. Brain glucose concentrations in poorly controlled diabetes mellitus as measured by high-field magnetic resonance spectroscopy. Metabolism 54, 1008–1013.

Shennan, D.B., Thomson, J., 2007. Estrogen regulation and ion dependence of taurine uptake by MCF-7 human breast cancer cells. Cell. Mol. Biol. Lett. 12, 396–406.

Shirayama, Y., Obata, T., Matsuzawa, D., Nonaka, H., Kanazawa, Y., Yoshitome, E., Ikehira, H., Hashimoto, K., Iyo, M., 2010. Specific metabolites in the medial prefrontal cortex are associated with the neurocognitive deficits in schizophrenia: a preliminary study. Neuroimage 49, 2783–2790.

Shughrue, P.J., Merchenthaler, I., 2000. Estrogen is more than just a "sex hormone": novel sites for estrogen action in the hippocampus and cerebral cortex. Front. Neuroendocrinol. 21, 95–101.

Tack, W., Wree, A., Schleicher, A., 1989. Local cerebral glucose utilization in the hippocampus of old rats. Histochemistry 92, 413–419.

Tayoshi, S.Y., Sumitani, S., Taniguchi, K., Shibuya-Tayoshi, S., Numata, S., Iga, J., Nakataki, M., Ueno, S., Harada, M., Ohmori, T., 2009. Metabolite changes and gender differences in schizophrenia using 3-Tesla proton magnetic resonance spectroscopy (^{1}H-MRS). Schizophr. Res. 108, 69–77.

Tkáč, I., Oz, G., Adriany, G., Uğurbil, K., Gruetter, R., 2009. In vivo ^{1}H NMR spectroscopy of the human brain at high magnetic fields: metabolite quantification at 4T vs. 7T. Magn. Reson. Med. 62, 868–879.

Tkáč, I., Rao, R., Georgieff, M.K., Gruetter, R., 2003. Developmental and regional changes in the neurochemical profile of the rat brain determined by in vivo ^{1}H NMR spectroscopy. Magn. Reson. Med. 50, 24–32.

VanGuilder, H.D., Yan, H., Farley, J.A., Sonntag, W.E., Freeman, W.M., 2010. Aging alters the expression of neurotransmission-regulating proteins in the hippocampal synaptoproteome. J. Neurochem. 113, 1577–1588.

Zacharoff, L., Tkáč, I., Song, Q., Tang, C., Bolan, P.J., Mangia, S., Henry, P.G., Li, T., Dubinsky, J.M., 2012. Cortical metabolites as biomarkers in the R6/2 model of Huntington's disease. J. Cereb. Blood Flow. Metab. 32, 502–514.